ACS APPLIED MATERIALS & INTERFACES

Research Article

www.acsami.org

# Selection of HBsAg-Specific DNA Aptamers Based on Carboxylated Magnetic Nanoparticles and Their Application in the Rapid and Simple Detection of Hepatitis B Virus Infection

Zhijiang Xi,[†,‡] Rongrong Huang,[†] Zhiyang Li,[†] Nongyue He,*[,†,§] Ting Wang,[†] Enben Su,[†,∥] and Yan Deng*[,†,§]

[†]State Key Laboratory of Bioelectronics, School of Biological Science and Medical Engineering, Southeast University, Nanjing 210096, P. R. China

[‡]School of Life and Science, Yangtze University, Jingzhou 434025, P. R. China

[§]Economical Forest Cultivation and Utilization of 2011 Collaborative Innovation Center in Hunan Province, Hunan Key Laboratory of Green Packaging and Application of Biological Nanotechnology, Hunan University of Technology, Zhuzhou 412007, P. R. China

[∥]Getein Biotechnology Co., Ltd., Nanjing 210000, P. R. China

Supporting Information

**ABSTRACT:** Aptamers are short single-stranded DNA or RNA oligonucleotides and can be selected from synthetic combinatorial libraries in vitro. They have a high binding affinity and specificity for their targets. Agarose gels, nitrocellulose membranes, and adsorptive microplates are often used as carriers to immobilize targets in the SELEX (systematic evolution of ligands by exponential enrichment) process, but the subsequent separation step is tedious and time-consuming. Therefore, we used magnetic nanoparticles (MNPs) as carriers to immobilize the target, hepatitis B surface antigen (HBsAg), which is convenient for fast magnetic separation. In this study, we first selected DNA aptamers against HBsAg by immobilizing HBsAg on the surface of carboxylated MNPs. The ssDNA library of each selection round was prepared by asymmetric PCR amplification for the next selection round. To obtain aptamer sequences, the final selected products were purified by gel electrophoresis, then cloned, and sequenced. DNA aptamers that specifically bind to HBsAg were successfully obtained after 13 selection rounds. The selected aptamers were used to construct a chemiluminescence aptasensor based on magnetic separation and immunoassay to detect HBsAg from pure protein or actual serum samples. There was a linear relationship between HBsAg concentration and chemiluminescent intensity in the range of 1−200 ng/mL. The aptasensor worked well even in the presence of interfering substances and was highly specific in the detection of HBsAg in serum samples, with a detection limit 0.1 ng/mL lower than the 0.5 ng/mL limit of an ELISA in use at the hospital. This aptasensor can contribute to better detection of hepatitis B virus infection.

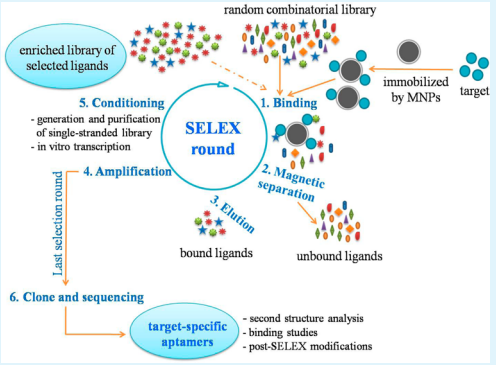


**KEYWORDS:** *aptamers, selection, SELEX, HBsAg, carboxylated magnetic nanoparticles, detection*

## INTRODUCTION

In 1990, a new method was described by Tuerk and Gold, using a combinatorial nucleic acid library to select RNA aptamers that bind very tightly and selectively to certain non-nucleic acid targets.[1] They selected the bacteriophage T4 DNA polymerase binding sequences from an RNA library randomized at specific positions, and called this selection procedure SELEX (systematic evolution of ligands by exponential enrichment). Two years later, Ellington et al.[2] reported that the single-stranded DNA sequences from a chemically synthesized random library were successfully selected. Since this early phase of the SELEX technology, it has become an important and widely used tool in molecular biological and medical research. Aptamers are short, single-stranded DNA or RNA segments of oligonucleotides, which can be selected from random combinatorial libraries by SELEX in vitro. Aptamers are viewed as artificial antibodies, but they possess several advantages when compared with antibodies: they are very stable, nonimmunogenic, nontoxic, simple to chemically modify, and easily and inexpensively produced.[3−5] Furthermore, aptamers have high binding affinities and specificities for their targets.[6−10] Binding of the aptamers to targets results from structure compatibility, stacking of aromatic rings, electrostatic and van der Waals interactions, hydrogen bondings, or a combination of these effects.[11−13]

Agarose gels, nitrocellulose membranes, and adsorptive microplates are often used as carriers to immobilize targets in

Received: February 6, 2015
Accepted: May 13, 2015
Published: May 13, 2015





DOI: 10.1021/acsami.5b01180
ACS Appl. Mater. Interfaces 2015, 7, 11215−11223

the SELEX process, but the subsequent separation step is tedious and time-consuming. However, using magnetic nanoparticles (MNPs) as carriers is convenient for fast magnetic separation.[14] In this work, we first selected DNA aptamers against hepatitis B virus surface antigen (HBsAg) using carboxylated MNPs as immobilized carriers and prepared an ssDNA library by asymmetric PCR amplification for the next selection round. In order to obtain aptamer sequences, the final selected products were PCR amplified and purified by gel electrophoresis and then were cloned and sequenced. A scheme of the in vitro selection of target-specific aptamers based on magnetic separation by SELEX is shown as Scheme 1. In

**Scheme 1. In Vitro Selection of Target-Specific Aptamers Based on Magnetic Separation by SELEX[a]**

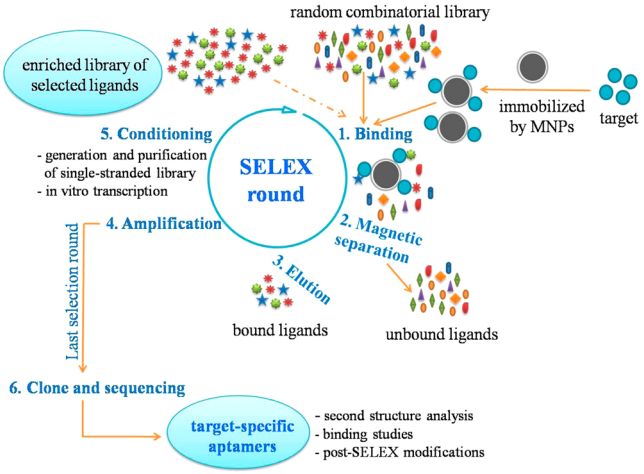


[a]The SELEX process is characterized by repetition of the five main steps: binding, magnetic separation, elution, amplification, and conditioning. The last SELEX round is terminated after the amplification step, and then the PCR products are cloned and sequenced.

conclusion, DNA aptamers that specifically bind to HBsAg were successfully selected after 13 SELEX rounds, and the secondary structures of aptamers were analyzed by DNAMAN software. To date, selection of DNA aptamers against HBsAg which can contribute to better detection and diagnosis of hepatitis B virus (HBV) infection has not been reported.

HBV infection, one of the most common viral infections in the world, is a global public health problem. It is one of the leading causes of chronic liver diseases, including chronic hepatitis, liver cirrhosis, hepatic failure, and hepatocellular carcinoma, especially in developing countries.[15−17] The virus is transmitted by blood and by body secretions, including saliva, tears, semen, and ascitic fluid contaminated with blood. However, the most common routes for transmission are through sexual contact and by mother to newborn infant. The genome of HBV is a small, circular, partially double-stranded DNA molecule containing four major open reading frames: pre-S/S, which encodes the surface antigen proteins of the virion envelope; pre-C/C, which encodes the core antigen of the nucleocapsid; X, which encodes the X protein; and P, which encodes the DNA polymerase of the virus.[18−20] HBsAg is the first virological marker to appear in the circulation and the most important marker of HBV infection, so the detection of HBsAg is a significant tool for the diagnosis of HBV infection.[21−23] HBsAg can be detected with available assay technology before clinical hepatitis develops, and typically as early as 6−8 weeks after the infection. There is a continuing need to develop more sensitive assays to shorten the period between the infection and the detection of infection markers, as well as to produce easy-to-perform assays for daily screening. Detection of HBsAg in serum samples is carried out commonly using an immunoassay that relies on two-site antibody−antigen interactions, such as an enzyme-linked immunosorbent assay (ELISA). However, ELISA is complex to perform and time-consuming, which leaves room for improvement. Here, we have developed a chemiluminescence aptasensor based on magnetic separation and immunoassay (Scheme 2), which allows rapid separation and sensitive detection of HBsAg in HBV infected serum.

## EXPERIMENTAL SECTION

**Materials and Reagents.** 1-Ethyl-3-(3-dimethyllaminopropyl) carbodiimide hydrochloride (EDC) and 3-aminopropyl triethoxysilane (APTES) were purchased from Sigma-Aldrich, Inc. (USA). Bovine serum albumin (BSA), 4-[2-hydroxyethyl]-1-piperazine ethanesulfonic acid (HEPES), tetramethyl benzidine (TMB), horseradish peroxidase (HRP) labeled streptavidin, ethylenediaminetetraacetic acid (EDTA), tris(hydroxymethyl)aminomethane (Tris), dithiothreitol (DTT), 3-(2′-spiroadamantane)-4-methoxy-4-(3″-phosphoryloxy)-phenyl-1,2-dioxetane (AMPPD), tween 20, guanidinium isothiocyanate, Taq DNA polymerase, and dNTP were purchased from Shanghai Sangon Biotech Co. Ltd. (Shanghai, China). HBsAg, primary mouse anti-HBsAg antibody, and secondary horse antimouse antibody labeled with alkaline phosphatase (ALP) were purchased from Shanghai Chao Yan Biotechnology Ltd. (Shanghai, China). Ethylene glycol, tetraethyl orthosilicate (TEOS), dimethylformamide (DMF), 2-*N*-morpholino ethanesulfonic acid (MES), and succinic anhydride were purchased from Nanjing Chemical Reagent Ltd. (Nanjing, China). The other chemical reagents were all of analytical grade from Nanjing Ronghua

**Scheme 2. Schematic Representation of the Construction of a Chemiluminescence Aptasensor Based on Magnetic Separation and Immunoassay**

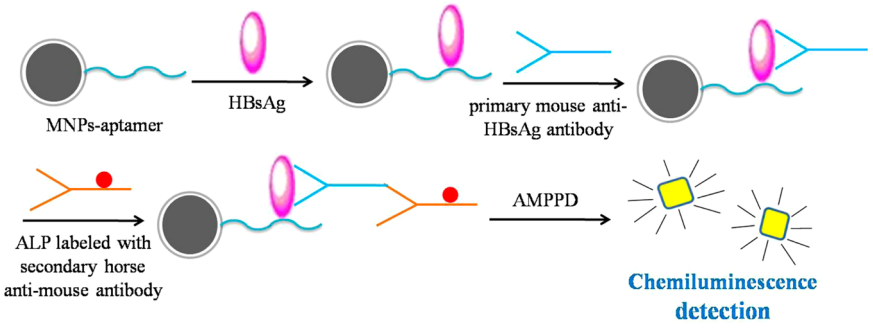



DOI: 10.1021/acsami.5b01180
ACS Appl. Mater. Interfaces 2015, 7, 11215−11223

Reagent Ltd. (Nanjing, China). Water used in the experiments was deionized (DI) prior to use.

The starting random ssDNA library and PCR amplification primers were synthesized by Shanghai Sangon Bioltech Co. Ltd. (Shanghai, China). The ssDNA library contained a 40-base central random sequence flanked by primer sites on either side. The sequences of these designed oligonucleotides were as follows:

ssDNA library: 5′-GGGAATTCGAGCTCGGTACC-40N-CTGCAGGCATGCAAGCTTGG-3′.

Forward primer: 5′-GGGAATTCGAGCTCGGTACC-3′.

Reverse primer: 5′-CCAAGCTTGCATGCCTGCAG-3′.

**Apparatus.** The transmission electron microscopy (TEM) images were obtained using a JEM-2100 TEM instrument (JEOL, Japan). The magnetic properties of $Fe_3O_4$@$SiO_2$ nanoparticles were measured with a vibrating sample magnetometer (Lakeshore Co., USA). A veriti 96-well thermal cycler (Applied Biosystems, USA) was used to PCR amplify the products of selection. The electrophoretogram was obtained using a JS-380A automated gel image analyzer (Shanghai Peiqing Science and Technology Ltd., China). The measurement of the affinity of aptamers for the target was performed using a Synergy HT microplate reader (BioTek, USA). The chemiluminescence detection of different concentrations of HBsAg was performed with an Enspire 2300 multilabel reader (PerkinElmer, USA).

**Preparation of $Fe_3O_4$@$SiO_2$ MNPs.** The $Fe_3O_4$ MNPs were synthesized via a modified solvothermal method.[24,25] Then the prepared $Fe_3O_4$ MNPs were coated with silica by the Stöber approach, which was appropriately modified to improve the dispersity of $Fe_3O_4$@$SiO_2$ nanoparticles. Briefly, 100 mL of the $Fe_3O_4$ MNPs at a concentration of 2 mg/mL were transferred into a three-neck flask. Under nitrogen, 2.5 mL of TEOS were divided into five equal parts and added to the $Fe_3O_4$ MNPs suspension. Then 2 mL of ammonia were added under vigorous stirring. The reaction system was kept at 35 °C for 6 h. Subsequently, the black precipitates of $Fe_3O_4$@$SiO_2$ MNPs were washed with absolute ethanol and DI water 6 times. Finally, $Fe_3O_4$@$SiO_2$ MNPs were redispersed in ethanol.

**Carboxyl Modification of $Fe_3O_4$@$SiO_2$ MNPs.**[26] The surface of silica can be easily modified by APTES under simple conditions. With vigorous stirring, 400 μL of APTES were added to 100 mg of $Fe_3O_4$@$SiO_2$ MNPs suspended in 40 mL of ethanol/water (volume ratio 39.8/0.2) solution. To enhance covalent bonding of the amino groups to the silica surface, the mixture was reacted for 5 h at room temperature. The black precipitates were washed 5 times with ethanol through magnetic separation, and the obtained amino-modified $Fe_3O_4$@$SiO_2$ MNPs were redispersed in 20 mL DMF.

The above-mentioned amino-modified $Fe_3O_4$@$SiO_2$ nanoparticles were added dropwise to 20 mL of 0.1 mol/L succinic anhydride solution and reacted for 24 h at room temperature and 180 rpm in an incubator shaker. The products were washed 5 times with DI water, and the obtained carboxylated $Fe_3O_4$@$SiO_2$ MNPs were redispersed in DI water.

**Coupling EDC-Activated, Carboxylated $Fe_3O_4$@$SiO_2$ MNPs with HBsAg.**[27−29] 10 mg of the above-mentioned carboxylated $Fe_3O_4$@$SiO_2$ MNPs were washed 3 times with MES buffer (25 mmol/L, pH 5.0), and the MNPs were dispersed into the buffer solution. Then 100 μL of freshly prepared 10 mg/mL EDC solution were added and shaken slowly for 30 min at 37 °C in order to activate the carboxy group on the surface of $Fe_3O_4$@$SiO_2$ MNPs. The products were washed 3 times with the above MES buffer to remove excess EDC. Finally, 300 μL of 1 mg/mL HBsAg solution were added to the above activated carboxylated MNPs solution, followed by slow shaking for 30 min at 37 °C. The products were washed 5 times with 0.01 mol/L (pH 7.4) of PBST solution to remove unreacted HBsAg, and the obtained HBsAg-immobilized $Fe_3O_4$@$SiO_2$ MNPs were kept at 4 °C. Through the measurement of the HBsAg concentration before and after the carboxylated $Fe_3O_4$@$SiO_2$ MNPs coupled with HBsAg, the coupling amount per mg of MNPs was calculated to be about 25 μg of HBsAg.

**Selection of DNA Aptamers Against HBsAg by SELEX.** At the start of SELEX, 1.5 mL of an empty Eppendorf tube was blocked with 1% BSA at 4 °C overnight. The random ssDNA library was denatured by heating at 95 °C for 5 min in a binding buffer (20 mmol/L HEPES, pH 7.35, 120 mmol/L NaCl, 5 mmol/L KCl, 1 mmol/L $CaCl_2$, and 1 mmol/L $MgCl_2$) and snap-cooled on ice for 10 min. The denatured ssDNA was then incubated with the above blocked Eppendorf tube for 60 min at 37 °C to eliminate the binding of sequences to the tube wall. The unbound sequences were incubated with the above-mentioned HBsAg-immobilized $Fe_3O_4$@$SiO_2$ MNPs in the binding buffer at 37 °C for specific periods (60 min for 1−4 rounds, 45 min for 5−8 rounds, and 30 min after 9 rounds), in order to gradually enhance selection pressure by reducing the reaction time. Through magnetic separation, sequences unbound by HBsAg-immobilized $Fe_3O_4$@$SiO_2$ were removed by extensive washing with washing buffer (the above binding buffer supplemented with 0.05% Tween 20). Bound sequences were then collected with eluting buffer (20 mmol/L Tris-HCl, 1 mmol/L DTT, and 4 mol/L guanidinium isothiocyanate, pH 8.3). The eluted ssDNA was amplified by asymmetric PCR to prepare an ssDNA library for the next selection round.[30] After 13 rounds, the final selected products were PCR amplified and purified by gel electrophoresis and were then cloned, sequenced, and characterized.

**Measurement of Binding Affinity.** The binding affinity of selected sequences in each SELEX round with HBsAg was determined by ELOSA (enzyme linked oligonucleotide adsorption test) at 450 nm with a microplate reader.[31] The eluted ssDNA of each selection round was PCR amplified with biotin-labeled forward primer and unlabeled reverse primer, and the PCR products were purified by using a PCR purification kit. Then 100 μL of 10 μg/mL purified PCR product were denatured and incubated with HBsAg-immobilized $Fe_3O_4$@$SiO_2$ MNPs. After magnetic separation, HRP-labeled streptavidin was added to the modified MNPs, with subsequent incubation for 30 min. The MNPs@HBsAg@aptamer@HRP composites were washed 5 times with PBST buffer, and then TMB solution was added to colorate for 15 min. Finally, the reaction was terminated by adding 0.5 mol/L of $H_2SO_4$ solution, and the absorption values were measured at 450 nm using a microplate reader.

**Construction of a Chemiluminescence Aptasensor.** The chemiluminescence method has the advantage of high sensitivity, wide linear dynamic range, relatively simple requirements, and inexpensive equipment needs.[32] In order to verify whether the selection of HBsAg-specific aptamers was successful or not, a chemiluminescence aptasensor based on magnetic separation and immunoassay was developed to detect HBsAg.

After selection, the obtained aptamers against HBsAg were amino-modified. The amino-modified aptamers were immobilized on the surface of the carboxylated $Fe_3O_4$@$SiO_2$ MNPs through a covalent bond to form the MNPs@aptamer composites. Then the composites were incubated with different concentrations of HBsAg solution, and subsequently, primary mouse anti-HBsAg antibody and secondary horse antimouse antibody labeled with alkaline phosphatase (ALP) were added to the incubating solution. The completed composites of MNPs@aptamer@HBsAg@primary antibody@secondary antibody@ALP were used to catalyze the chemiluminescence of AMPPD after magnetic separation. The chemiluminescence detection of different concentrations of HBsAg from pure protein or actual serum samples was performed using an Enspire 2300 multilabel reader.

**Test of Specificity and Sensitivity.** The specifitity of selected aptamers for HBsAg in serum samples was tested using normal serum, hepatitis A serum, hepatitis C serum, and mixed serums of hepatitis A, B, and C as controls. HBsAg in positive hepatitis B serum was diluted to concentrations of 100, 50, 10, 1, and 0.1 ng/mL. A 40 μL aliquot of each of the serum samples was used in every test. Each experiment or treatment was repeated 3 times.

## RESULTS AND DISCUSSION

**Characterization of $Fe_3O_4$@$SiO_2$ MNPs.** The morphology and size of the obtained $Fe_3O_4$@$SiO_2$ nanoparticles were observed and analyzed by TEM as shown in Figure 1. From TEM images, $Fe_3O_4$ MNPs can be observed as dark spheres, and the $SiO_2$ shells, as gray layers. The $Fe_3O_4$@$SiO_2$ nanoparticles were displayed in a spherical morphology and



DOI: 10.1021/acsami.5b01180
ACS Appl. Mater. Interfaces 2015, 7, 11215−11223

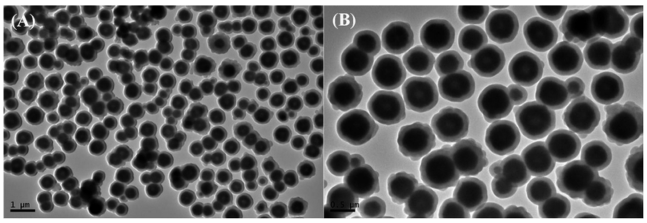


**Figure 1.** TEM images of $Fe_3O_4$@$SiO_2$ MNPs. (A) In the scope of 1 $\mu$m. (B) In the scope of 0.5 $\mu$m.

homogeneous size. The average diameters of the $Fe_3O_4$ and $Fe_3O_4$@$SiO_2$ nanoparticles were about 450 and 550 nm, respectively. They had good dispersity, which made them excellent immobilized carriers for other molecules.[33−36] In recent years, various materials have been used as coatings for $Fe_3O_4$ nanoparticles, including noble metals, metal oxides, silica, and organic polymers.[37−40] Among these coating materials, silica is very promising because it can prevent $Fe_3O_4$ cores from directly contacting liquid media, and most importantly, the surface chemistry of a silica shell is compatible with many chemicals and molecules for bioconjugation.[41] The surface of silica is easily modified with various chemical groups, such as amino, carboxyl, sulfhydryl, and aldehyde groups.[42−45]

The magnetic properties of $Fe_3O_4$@$SiO_2$ nanoparticles were measured using a vibrating sample magnetometer (VSM). The results showed that the $Fe_3O_4$@$SiO_2$ MNPs had excellent magnetic properties (Figure 2), with a saturation magnetization

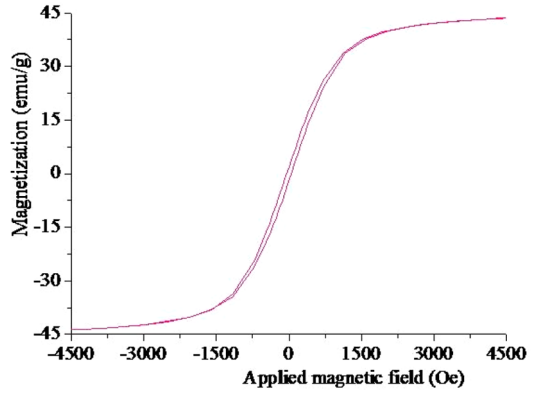


**Figure 2.** Hysteresis loop of $Fe_3O_4$@$SiO_2$ MNPs.

of 43.86 emu/g. Fast magnetic separation, utilizing the magnetic properties of $Fe_3O_4$@$SiO_2$ nanoparticles, is convenient and widely used in diverse applications.[46−51]

**Optimization of Asymmetric PCR Conditions.** One of the most common methods for generating ssDNA in DNA aptamer selection is asymmetric PCR, which produces ssDNA due to the unequal concentration of forward and reverse primers used in the reaction system. The important amplification conditions of asymmetric PCR, such as the amount of Taq DNA polymerase, the proportion of forward and reverse primers, the annealing temperature, and the amplification cycle number, were optimized, and the results are shown in Figure S1 (Supporting Information). The optimization was accomplished by examining one variable at a time while maintaining the other variables constant. The four variables were kept constant respectively as follows: 1.5 U of Taq DNA polymerase, a 100:1 ratio of forward primer to reverse primer, an annealing temperature of 66 °C, and 35 amplification cycles. As shown in Figure S1A, there was no electrophoresis band without Taq DNA polymerase, the band was weak when the polymerse dosage was low, and the band was bright accompanied by a weak, nonspecific band when the polymerse dosage was more than 1.5 U. Based on this, the optimized dosage of Taq DNA polymerase was selected to be 1.5 U. As shown in Figure S1B, the optimized proportion of forward primer to reverse primer was 90:1. As shown in Figure S1C, there were bright bands for each annealing temperature, but there were weak, nonspecific bands for 60 to 66 °C. Therefore, the best annealing temperature was selected to be 68 °C. Finally as shown in Figure S1D, no band was observed when the amplification cycle number was 15 or 20, but the bands were bright when the cycle number was more than 30. However, nonspecific amplification was apparent when the cycle number was increased further. Therefore, the best cycle number was determined to be 30. In sum, the optimized amplification conditions in a 50 $\mu$L PCR reaction system were the following: 1.5 U of Taq DNA polymerase, a 90:1 ratio of forward primer to reverse primer, an annealing temperature at 68 °C, and 30 amplification cycles. Furthermore, the type of template DNA was from a synthetic DNA library for the first selection round and was a symmetric PCR product from the aptamer pool for the other rounds. The amount of template DNA was about 10 ng in a 50 $\mu$L PCR reaction system for each selection round, which was determined by pre-experiment.

**Electrophoretogram of the Products of Asymmetric PCR.** Asymmetric PCR has become the most common procedure for producing ssDNA in DNA aptamer selection, because it is more economical and less tedious than other methods, involving the same parameters for PCR amplification as the SELEX process (except for primer ratios). In this study, the products of asymmetric PCR in each selection round were detected by electrophoresis with a 2% agarose gel, shown in Figure S2 (Supporting Information). The result showed that HBsAg-specific DNA sequences were successfully selected and that ssDNA pools were amplified in each SELEX round, strongly suggesting selection success of these aptamers.

**Measurement of Binding Affinity.** In each SELEX round, the binding affinity of selected sequences for the HBsAg target was measured by ELOSA, as shown in Figure S3 (Supporting Information). At the beginning, the absorption value increased rapidly with an increase in the selection round. After 11 rounds, the value increased very slowly, which showed that the binding affinity was nearing its maximum. Therefore, the whole SELEX process was terminated after the 13th round.

**Sequencing Map of Selected Aptamers.** The selected products of the 13th round were amplified by PCR and purified by gel electrophoresis. Then the purified PCR products were cloned and sequenced. Fifteen randomly picked clones were sequenced, and three different aptamers were obtained. The sequences of most aptamers were the same as those shown in Figure 3A, confirming that a high binding affinity of DNA sequences to the HBsAg target was achieved after 13 selection rounds. The aptamers shown in Figure 3A,B,C were named H01, H02, and H03 respectively.

**Analysis of Secondary Structure of Selected Aptamers.** Aptamers have specific and complex three-dimensional shapes, characterized by stems, hairpins, bulges, loops, pseudoknots, triplexes, or quadruplexes.[52] The secondary structures of selected aptamers against HBsAg were analyzed by DNAMAN software. The three different aptamers all have a


DOI: 10.1021/acsami.5b01180
ACS Appl. Mater. Interfaces 2015, 7, 11215−11223

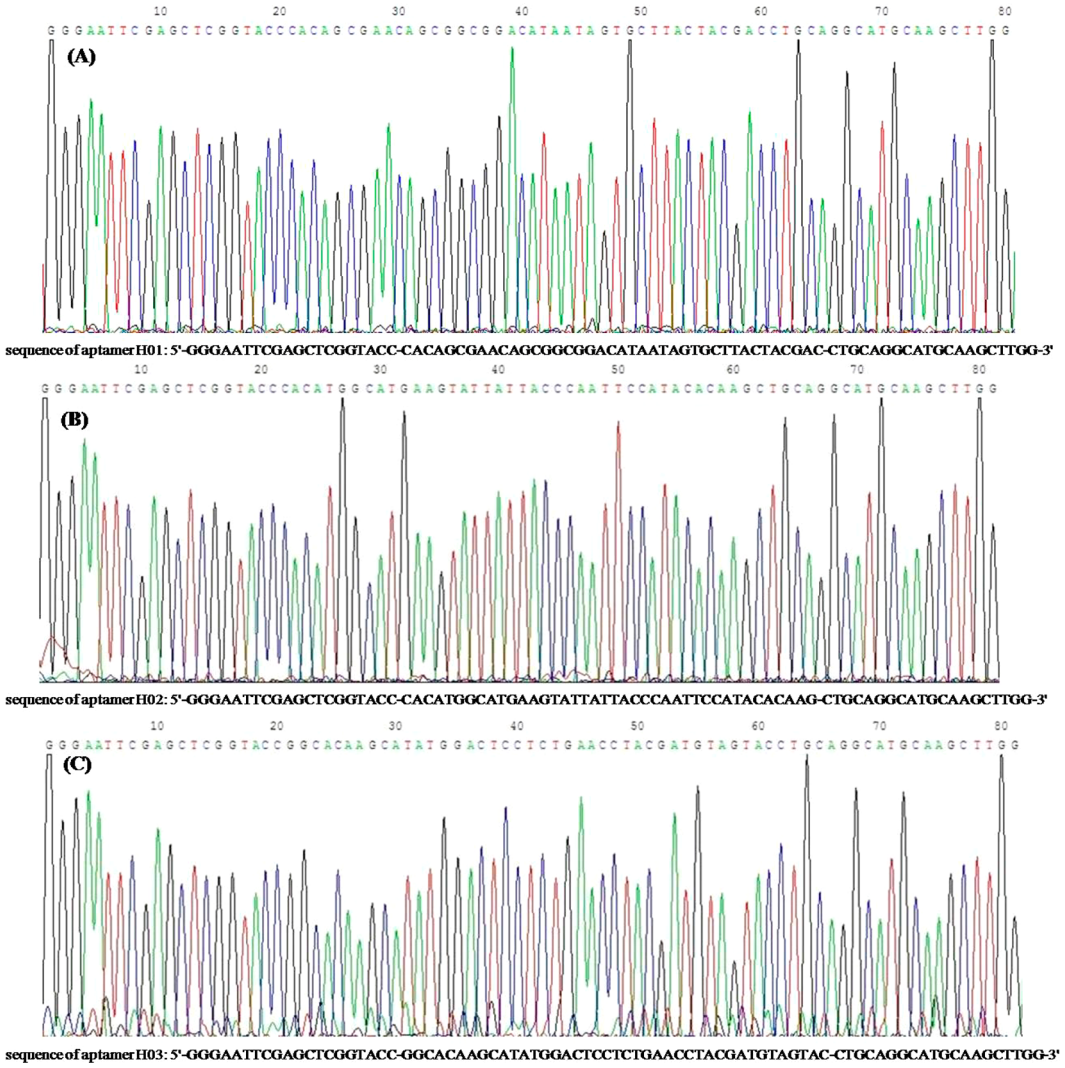


**Figure 3.** Sequencing map of selected aptamers against HBsAg. (A) Aptamer H01, showing sequence similarity with most selected aptamers. (B) Aptamer H02. (C) Aptamer H03.

loop−hairpin structure as shown in the red rectangular area in Figure 4. Aptamer H01 has two combined loop-hairpin structures that form a loop−hairpin−loop−hairpin composite structure; aptamer H02 has two separate loop−hairpin structures; and aptamer H03 has only one loop−hairpin structure. Based on their three-dimensional structures, aptamers can bind well to a wide variety of targets, from single molecules to complex mixtures or even whole cells.[53−62] The diversity of targets used in the SELEX process suggests that aptamers can be successfully selected against virtually any target.

**Optimization of Detection Conditions.** Chemiluminescence aptasensors have attracted increasing attention and have become an important branch of aptasensor study. The three selected aptamers were all used to construct chemiluminescence aptasensors based on magnetic separation and immunoassay to detect HBsAg in samples. As shown in Figure S4 (Supporting Information), the binding affinity (determined by ELOSA, too) of the H01 aptamer was the highest, so it was selected for further use in the detection of HBsAg. The three different aptamers against HBsAg all have a loop−hairpin structure, but aptamer H01 has two combined loop−hairpin structures that form a loop−hairpin−loop−hairpin composite structure, which may be the reason why the binding affinity of H01 is higher than either H02 and H03.

The conditions for the detection of HBsAg were optimized (Figure S5, Supporting Information), including the amount of aptamer, the amount of MNPs, the amount of primary mouse anti-HBsAg antibody, and the amount of secondary horse antimouse antibody labeled with alkaline phosphatase (ALP).

The amino-modified aptamer against HBsAg was immobilized on the surface of the carboxyl-modified $Fe_3O_4$@$SiO_2$ particles. As shown in Figure S5A, the chemiluminescent intensity gradually increased as the amount of aptamer increased, but when the amount of aptamer reached 200 pmol per mg MNPs, the increase in chemiluminescent intensity slowed substantially. Based on this finding, the best amount of aptamer was selected to be 200 pmol per mg MNPs. As shown in Figure S5B, the chemiluminescent intensity also increased first and then decreased with an increasing amount of $Fe_3O_4$@$SiO_2$ MNPs. When the chemiluminescent intensity reached its maximum, excess MNPs would cause a decrease in this intensity because of a masking effect of the $Fe_3O_4$ nanoparticles. Based on this result, the best amount of MNPs was selected to be 400 $\mu$g. The solutions of both primary mouse anti-HBsAg antibody and secondary horse antimouse antibody were diluted


DOI: 10.1021/acsami.5b01180
ACS Appl. Mater. Interfaces 2015, 7, 11215−11223

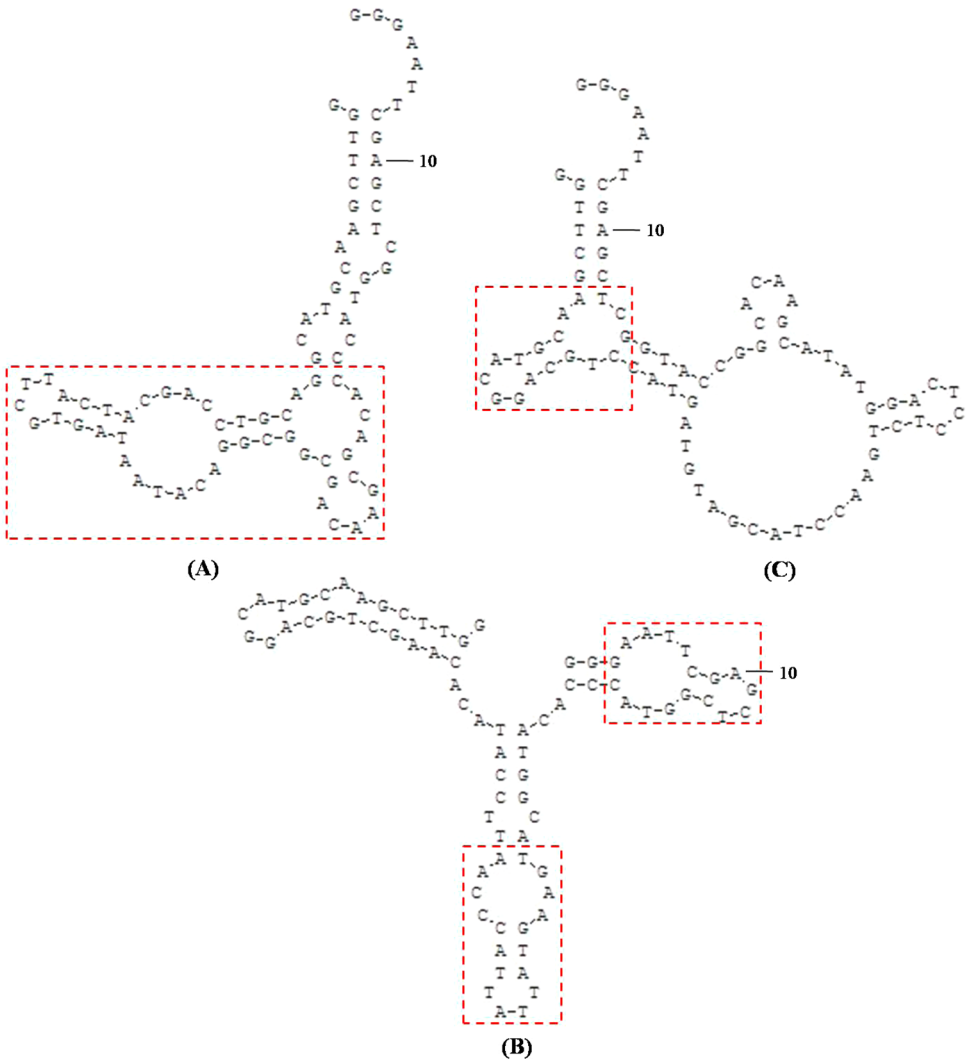


**Figure 4.** Secondary structures of selected aptamers against HBsAg. (A) Aptamer H01. (B) Aptamer H02. (C) Aptamer H03.

individually, and 40 $\mu$L of the diluent were used in each experiment. As shown in Figure S5C,D, the chemiluminescent intensities increased gradually and then slowed with an increase in primary and secondary antibody. The optimal amounts for both primary antibody and secondary antibody were determined to be 0.4 $\mu$g.

**Detection of Pure HBsAg.** The pure protein of HBsAg was prepared in various dilutions, and then the chemiluminescent intensity was measured using our newly developed chemiluminescence aptasensor. There was a linear relationship between the concentration of HBsAg and the chemiluminescent intensity in the range of 1−200 ng/mL (Figure 5), indicating success in selecting aptamers against HBsAg. The regression equation for this relationship was $y = 28.7x + 1082$, with a regression coefficient of 0.997.

**Detection of HBsAg in Actual Serum Samples.** Positive serum samples containing HBsAg were obtained from the Second Hospital of Nanjing, China. Using our constructed chemiluminescence aptasensor, 35 serum samples were tested. DI water was used as the blank, and the normal serum was used as a negative control. The results were roughly in line with results from the ELISA used at the hospital (Table S1, Supporting Information). Figure 6 shows the result from the detection of several HBV-positive serums. Concentrations of

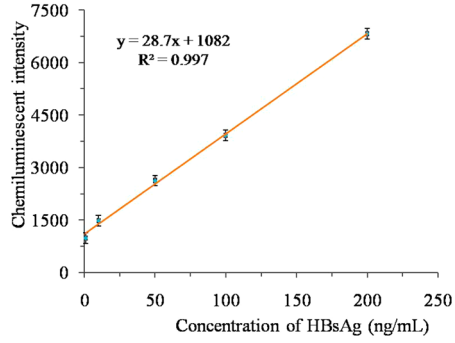


**Figure 5.** Linear relationship between the concentration of HBsAg and the chemiluminescent intensity in the range of 1−200 ng/mL.

HBsAg were 0.1, 1, 10, 50, and 100 ng/mL for five clinical samples. The detection limit of 0.1 ng/mL of HBsAg was estimated ($Q = 2.18 > 2.1$) and was found to be lower than the 0.5 ng/mL limit of the ELISA in use at the hospital.

**Specificity of Aptamer to Target HBsAg.** In order to assess the specificity of the selected aptamer to the serum samples containing HBsAg, experiments were conducted on the following controls: normal serum (negative control), hepatitis A serum, hepatitis C serum, and mixed serum of hepatitis A, B,


DOI: 10.1021/acsami.5b01180
ACS Appl. Mater. Interfaces 2015, 7, 11215−11223

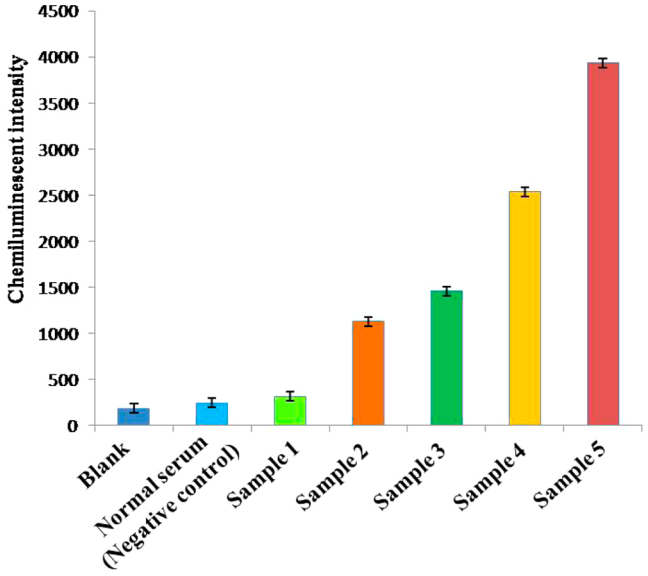


**Figure 6.** Detection of different HBsAg concentrations in hepatitis B serum. HBsAg concentrations of samples 1 to 5 were 0.1, 1, 10, 50, and 100 ng/mL, respectively.

and C. And DI water is used as the blank instead of serum. From Figure 7, the result showed that the chemiluminescent

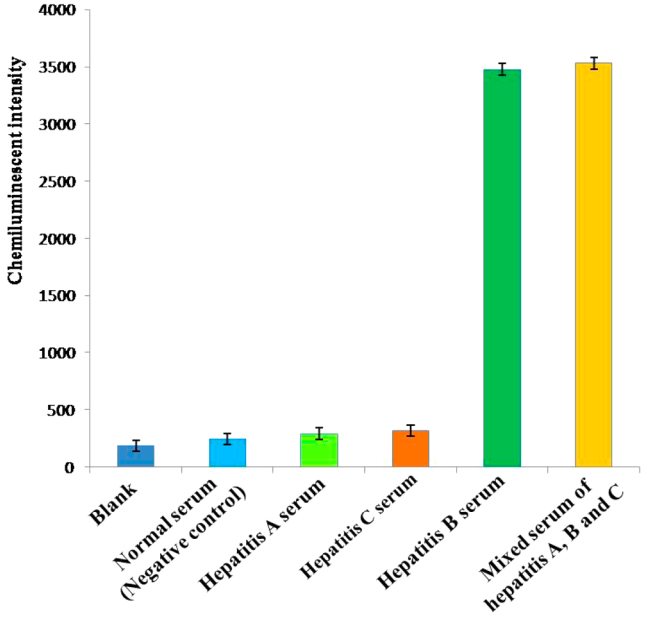


**Figure 7.** Specificity of the selected aptamer for different serums.

signals of normal serum, hepatitis A serum, and hepatitis C serum were very low and close to the blank. On exposure to HBV-positive serum, however, a significant increase in chemiluminescent intensity was observed, indicating that the selected aptamer had high specificity toward the target molecule. The cross-sensitivity of the chemiluminescence aptasensor in a mixture of equal volumes of hepatitis A, B, and C serums was also examined. The results showed that there was no significant change observed in the mixed serums of hepatitis A, B, and C compared with hepatitis B serum. This indicated that hepatitis A serum and hepatitis C serum had an almost negligible influence on the detection of hepatitis B serum, suggesting that the aptasensor would work well even in the presence of interfering substances such as coinfections. In sum, this aptasensor demonstrated sufficient specificity for the detection of HBsAg in serum samples.

## CONCLUSIONS

We first selected HBsAg-specific DNA aptamers by immobilizing HBsAg on the surface of carboxylated MNPs, making it possible to utilize magnetic separation in the SELEX process. After 13 selection rounds, three different aptamers were successfully selected in vitro. The secondary structures of selected aptamers were analyzed by DNAMAN software, the result of which showed that the three different aptamers all have a loop−hairpin structure. Moreover, a chemiluminescence aptasensor based on magnetic separation and immunoassay was constructed to detect HBsAg from pure protein or actual serum samples. There was a linear relationship between the concentration of HBsAg and the chemiluminescent intensity in the range of 1−200 ng/mL using aptamer H01. The aptasensor worked well and was highly specific for the detection of HBsAg in serum samples. The detection limit was 0.1 ng/mL, which was lower than the 0.5 ng/mL limit of the ELISA used at the hospital. However, ELISA is complex to perform and time-consuming. The chemiluminescence aptasensor based on magnetic separation and immunoassay allows rapid separation and sensitive detection of HBsAg in HBV infected serum. This aptasensor has the potential for wide clinical application in the diagnosis of HBV infection, and this method can also be applied to detect other molecules associated with disease.

## ASSOCIATED CONTENT

### Supporting Information

Additional table and figures as noted in text. The Supporting Information is available free of charge on the ACS Publications website at DOI: 10.1021/acsami.5b01180.

## AUTHOR INFORMATION

### Corresponding Authors

*Phone/Fax: +86-25-83790885. E-mail: nyhe@seu.edu.cn (N.H.).

*Phone/Fax: +86-25-83790885. E-mail: hndengyan@126.com (Y.D.).

### Notes

The authors declare no competing financial interest.

## ACKNOWLEDGMENTS

This research was financially supported by the National Key Program for Developing Basic Research (Nos. 2014CB744501 and 2010CB933903), the Chinese National Key Project of Science and Technology (2013ZX10004103-002), the NSFC (61271056, 61471168, 61201100, and 61201033), Open Research Fund by State Key Laboratory of Bioelectronics, Southeast University, China, the 11th Foundation for Jiangsu Provincial Science and Technology Innovation & Transformation of Health Science and Technology Achievements of 2012 (BL2012067), the Talents Planning of Six Summit Fields of Jiangsu Province (WSN-056), the Economical Forest Cultivation and Utilization of 2011 Collaborative Innovation Center in Hunan Province [(20130) 448], and College Postgraduate Research and Innovation Project in Jiangsu province, China (CXLX0146).



DOI: 10.1021/acsami.5b01180
ACS Appl. Mater. Interfaces 2015, 7, 11215−11223

## REFERENCES


(1) Tuerk, C.; Gold, L. Systematic Evolution of Ligands by Exponential Enrichment RNA Ligands to Bacteriophage T4 DNA Polymerase. *Science* **1990**, *249*, 505−510.

(2) Ellington, A. D.; Szostak, J. W. Selection in Vitro of Single-stranded DNA Molecules that Fold into Specific Ligand-binding Structures. *Nature* **1992**, *355*, 850−852.

(3) Nimjee, S. M.; Rusconi, C. P.; Harrington, R. A.; Sullenger, B. A. The Potential of Aptamers as Anticoagulants. *Trends Cardiovas. Med.* **2005**, *15*, 41−45.

(4) Jayasena, S. D. Aptamers: an Emerging Class of Molecules that Rival Antibodies in Diagnostics. *Clin. Chem.* **1999**, *45*, 1628−1650.

(5) Dollins, C. M.; Nair, S.; Sullenger, B. A. Aptamers in Immunotherapy. *Hum. Gene Ther.* **2008**, *19*, 443−450.

(6) Göringer, H. U.; Homann, M.; Lorger, M. In Vitro Selection of High-affinity Nucleic Acid Ligands to Parasite Target Molecules. *Int. J. Parasitol.* **2003**, *33*, 1309−1317.

(7) Hamula, C.; Zhang, H. Q.; Guan, L. L.; Li, X. F.; Le, X. C. Selection of Aptamers Against Live Bacterial Cells. *Anal. Chem.* **2008**, *80*, 7812−7819.

(8) Tracy, R. B.; Kowalczykowski, S. C. In Vitro Selection of Preferred DNA Pairing Sequences by the *Escherichia coli* RecA Protein. *Genes Dev.* **1996**, *10*, 1890−1903.

(9) Conrad, R. C.; Giver, L.; Tian, Y.; Ellington, A. D. In Vitro Selection of Nucleic Acid Aptamers that Bind Proteins. *Comb. Chem.* **1996**, *267*, 336−367.

(10) Moreno, M.; Rincon, E.; Pineiro, D.; Fernandez, G.; Domingo, A.; Jimenez-Ruiz, A.; Salinas, M.; Gonzalez, V. M. Selection of Aptamers Against KMP-11 Using Colloidal Gold During the SELEX Process. *Biochem. Biophys. Res. Commun.* **2003**, *308*, 214−218.

(11) Jhaveri, S.; Rajendran, M.; Ellington, A. D. In Vitro Selection of Signaling Aptamers. *Nat. Biotechnol.* **2000**, *18*, 1293−1297.

(12) Kulbachinskiy, A. V. Methods for Selection of Aptamers to Protein Targets. *Biochemistry-Moscow* **2007**, *72*, 1505−1518.

(13) Han, S. R.; Lee, S. W. In Vitro Selection of RNA Aptamer Specific to *Salmonella typhimurium*. *J. Microbiol. Biotechnol.* **2013**, *23*, 878−884.

(14) Lou, X. H.; Qian, J. R.; Xiao, Y.; Viel, L.; Gerdon, A. E.; Lagally, E. T. Micromagnetic Selection of Aptamers in Microfluidic Channels. *Proc. Natl. Acad. Sci. U.S.A.* **2009**, *106*, 2989−2994.

(15) Orito, E.; Ichida, T.; Sakugawa, H.; Sata, M.; Horiike, N.; Hino, K.; Okita, K.; Okanoue, T.; Iino, S.; Tanaka, E. Geographic Distribution of Hepatitis B Virus (HBV) Genotype in Patients with Chronic HBV Infection in Japan. *Hepatology* **2001**, *34*, 590−594.

(16) Bielawski, K. P.; Stalke, P. Molecular Epidemiology of Chronic Hepatitis B Virus Infection in Northern Poland. *J. Clin. Virol.* **2005**, *34*, S63−S69.

(17) Lavanchy, D. Worldwide Epidemiology of HBV Infection, Disease Burden, and Vaccine Prevention. *J. Clin. Virol.* **2005**, *34*, S1−S3.

(18) Ganem, D.; Varmus, H. The Molecular Biology of the Hepatitis B Viruses. *Annu. Rev. Biochem.* **1987**, *56*, 651−693.

(19) Seeger, C.; Ganem, D.; Varmus, H. E. Biochemical and Genetic Evidence for the Hepatitis B Virus Replication Strategy. *Science* **1986**, *232*, 477−484.

(20) Mason, W. S.; Taylor, J. M. Experimental Systems for the Study of Hepadnavirus and Hepatitis Delta Virus Infections. *Hepatology* **1989**, *9*, 635−645.

(21) Lin, T. M.; Chen, C. J.; Wu, M. M.; Yang, C. S.; Chen, J. S.; Lin, C. C.; Kwang, T. Y.; Hsu, S. T.; Lin, S. Y.; Hsu, L. C. Hepatitis B Virus Markers in Chinese Twins. *Anticancer Res.* **1989**, *9*, 737−741.

(22) Zhevachevsky, N. G.; Nomokonova, N. Y.; Beklemishev, A. B.; Belov, G. F. Dynamic Study of HBsAg and HBeAg in Saliva Samples from Patients with Hepatitis B Infection: Diagnostic and Epidemiological Significance. *J. Med. Virol.* **2000**, *61*, 433−438.

(23) Vranckx, R.; Alisjahbana, A.; Meheus, A. Hepatitis B Virus Vaccination and Antenatal Transmission of HBV Markers to Neonates. *J. Viral Hepatitis* **1999**, *6*, 135−139.

(24) Jiang, H. R.; Zeng, X.; Xi, Z. J.; Liu, M.; Li, C. Y.; Li, Z. Y.; Jin, L.; Wang, Z. F.; Deng, Y.; He, N. Y. Improvement on Controllable Fabrication of Streptavidin-modified Three-Layer Coreshell $Fe_3O_4$@$SiO_2$@Au Magnetic Nanocomposites with Low Fluorescence Background. *J. Biomed. Nanotechnol.* **2013**, *9*, 674−684.

(25) He, L.; Li, Z. Y.; Fu, J.; Wang, F.; Ma, C.; Deng, Y.; Shi, Z. Y.; Wang, H.; He, N. Y. Preparation of $SiO_2$/(PMMA/$Fe_3O_4$) Nanoparticles Using Linolenic Acid as Crosslink Agent for Nucleic Acid Detection Using Chemiluminescent method. *J. Nanosci. Nanotechnol.* **2011**, *11*, 2256−2262.

(26) An, Y. Q.; Chen, M.; Xue, Q. J.; Liu, W. M. Preparation and Self-assembly of Carboxylic Acid-Functionalized Silica. *J. Colloid Interface Sci.* **2007**, *311*, 507−513.

(27) Akram, M.; Stuart, M. C.; Wong, D. K. Direct Application Strategy to Immobilise a Thioctic Acid Self-Assembled Monolayer on a Gold Electrode. *Anal. Chim. Acta* **2004**, *504*, 243−251.

(28) Berggren, C.; Johansson, G. Capacitance Measurements of Antibody-Antigen Interactions in a Flow System. *Anal. Chem.* **1997**, *69*, 3651−3657.

(29) Lee, C. F.; Young, T. H.; Huang, Y. H.; Chiu, W. Y. Synthesis and Properties of Polymer Latex with Carboxylic Acid Functional Groups for Immunological Studies. *Polymer* **2000**, *41*, 8565−8571.

(30) Marimuthu, C.; Tang, T. H.; Tominaga, J.; Tan, S. C.; Gopinath, S. C. Single-Stranded DNA (ssDNA) Production in DNA Aptamer Generation. *Analyst* **2012**, *137*, 1307−1315.

(31) Bernard, J.; Schappacher, M.; Deffieux, A.; Viville, P.; Lazzaroni, R.; Charles, M. H.; Charreyre, M. T.; Delair, T. Water-Soluble Dendrigrafts Bearing Saccharidic Moieties: Elaboration and Application to Enzyme Linked Oligosorbent Assay (ELOSA) Diagnostic Tests. *Bioconjugate Chem.* **2006**, *17*, 6−14.

(32) Zhao, L. X.; Sun, L.; Chu, X. G. Chemiluminescence Immunoassay. *TrAC, Trends Anal. Chem.* **2009**, *28*, 404−415.

(33) Chang, Q.; Zhu, L. H.; Jiang, G. D.; Tang, H. Q. Sensitive Fluorescent Probes for Determination of Hydrogen Peroxide and Glucose Based on Enzyme-Immobilized Magnetite/Silica Nanoparticles. *Anal. Bioanal. Chem.* **2009**, *395*, 2377−2385.

(34) Huang, J.; Zhao, R.; Wang, H.; Zhao, W. Q.; Ding, L. Y. Immobilization of Glucose Oxidase on $Fe_3O_4$/$SiO_2$ Magnetic Nanoparticles. *Biotechnol. Lett.* **2010**, *32*, 817−821.

(35) Makhluf, S. B. D.; Abu-Mukh, R.; Rubinstein, S.; Breitbart, H.; Gedanken, A. Modified PVA-$Fe_3O_4$ Nanoparticles as Protein Carriers into Sperm Cells. *Small* **2008**, *4*, 1453−1458.

(36) Tang, Y. J.; Zou, J.; Ma, C.; Ali, Z.; Li, Z. Y.; Li, X. L. Highly Sensitive and Rapid Detection of *Pseudomonas Aeruginosa* Based on Magnetic Enrichment and Magnetic Separation. *Theranostics* **2013**, *3*, 85−92.

(37) Chen, C. T.; Chen, Y. C. $Fe_3O_4$/$TiO_2$ Core/Shell Nanoparticles as Affinity Probes for the Analysis of Phosphopeptides Using $TiO_2$ Surface-Assisted Laser Desorption/Ionization Mass spectrometry. *Anal. Chem.* **2005**, *77*, 5912−5919.

(38) Xie, J.; Xu, C. J.; Kohler, N.; Hou, Y. L.; Sun, S. H. Controlled PEGylation of Monodisperse $Fe_3O_4$ Nanoparticles for Reduced Non-specific Uptake by Macrophage Cells. *Adv. Mater.* **2007**, *19*, 3163−3166.

(39) Wang, L. Y.; Luo, J.; Fan, Q.; Suzuki, M.; Suzuki, I. S.; Engelhard, M. H.; Lin, Y. H.; Kim, N.; Wang, J. Q. Monodispersed Core-Shell $Fe_3O_4$@Au Nanoparticles. *J. Phys. Chem. B* **2005**, *109*, 21593−21601.

(40) He, Y. P.; Wang, S. Q.; Li, C. R.; Miao, Y. M.; Wu, Z. Y.; Zou, B. S. Synthesis and Characterization of Functionalized Silica-Coated $Fe_3O_4$ Superparamagnetic Nanocrystals for Biological Applications. *J. Phys. D: Appl. Phys.* **2005**, *38*, 1342−1350.

(41) Morel, A. L.; Nikitenko, S. I.; Gionnet, K.; Wattiaux, A.; Lai-Kee-Him, J.; Labrugere, C.; Chevalier, B.; Deleris, G.; Petibois, C.; Brisson, A. Sonochemical Approach to the Synthesis of $Fe_3O_4$@$SiO_2$ Core−Shell Nanoparticles with Tunable Properties. *ACS Nano* **2008**, *2*, 847−856.

(42) De Palma, R.; Trekker, J.; Peeters, S.; Van Bael, M. J.; Bonroy, K.; Wirix-Speetjens, R.; Reekmans, G.; Laureyn, W.; Borghs, G.; Maes,




DOI: 10.1021/acsami.5b01180
*ACS Appl. Mater. Interfaces* 2015, 7, 11215−11223

G. Surface Modification Gamma-$Fe_2O_3$@$SiO_2$ Magnetic Nanoparticles for the Controlled Interaction with Biomolecules. *J. Nanosci. Nanotechnol.* **2007**, *7*, 4626−4641.
(43) Khosroshahi, M. E.; Ghazanfari, L. Amino Surface Modification of $Fe_3O_4$/$SiO_2$ Nanoparticles for Bioengineering Applications. *Surf. Eng.* **2011**, *27*, 573−580.
(44) Mohammadi, A.; Barikani, M.; Barmar, M. Effect of Surface Modification of $Fe_3O_4$ Nanoparticles on Thermal and Mechanical Properties of Magnetic Polyurethane Elastomer Nanocomposites. *J. Mater. Sci.* **2013**, *48*, 7493−7502.
(45) Yan, H.; Zhang, J. C.; You, C. X.; Song, Z. W.; Yu, B. W.; Shen, Y. Surface Modification of $Fe_3O_4$ Nanoparticles and Their Magnetic Properties. *Int. J. Miner., Metall. Mater.* **2009**, *16*, 226−229.
(46) Park, M.; Seo, S.; Lee, I. S.; Jung, J. H. Ultraefficient Separation and Sensing of Mercury and Methylmercury Ions in Drinking Water by Using Aminonaphthalimide-Functionalized $Fe_3O_4$@$SiO_2$ Core/Shell Magnetic Nanoparticles. *Chem. Commun.* **2010**, *46*, 4478−4480.
(47) Shao, H. L.; Min, C.; Issadore, D. A.; Liong, M.; Yoon, T. J.; Weissleder, R. Magnetic Nanoparticles and MicroNMR for Diagnostic Applications. *Theranostics* **2012**, *2*, 55−65.
(48) Shao, M. F.; Ning, F. Y.; Zhao, J. W.; Wei, M.; Evans, D. G.; Duan, X. Preparation of $Fe_3O_4$@$SiO_2$@Layered Double Hydroxide Core−Shell Microspheres for Magnetic Separation of Proteins. *J. Am. Chem. Soc.* **2012**, *134*, 1071−1077.
(49) Simeonidis, K.; Gkinis, T.; Tresintsi, S.; Martinez-Boubeta, C.; Vourlias, G.; Tsiaoussis, I.; Stavropoulos, G.; Mitrakas, M.; Angelakeris, M. Magnetic Separation of Hematite-Coated $Fe_3O_4$ Particles Used as Arsenic Adsorbents. *Chem. Eng. J.* **2011**, *168*, 1008−1015.
(50) Yavuz, C. T.; Mayo, J. T.; William, W. Y.; Prakash, A.; Falkner, J. C.; Yean, S.; Cong, L.; Shipley, H. J.; Kan, A.; Tomson, M. Low-Field Magnetic Separation of Monodisperse $Fe_3O_4$ Nanocrystals. *Science* **2006**, *314*, 964−967.
(51) Xie, J.; Jon, S. Y. Magnetic Nanoparticle-Based Theranostics. *Theranostics* **2012**, *2*, 122−124.
(52) Stoltenburg, R.; Reinemann, C.; Strehlitz, B. SELEX - A (R)evolutionary Method to Generate High-Affinity Nucleic Acid Ligands. *Biomol. Eng.* **2007**, *24*, 381−403.
(53) Lauhon, C. T.; Szostak, J. W. RNA Aptamers that Bind Flavin and Nicotinamide Redox Cofactors. *J. Am. Chem. Soc.* **1995**, *117*, 1246−1257.
(54) Yang, Q.; Goldstein, I. J.; Mei, H. Y. DNA Ligands that Bind Tightly and Selectively to Cellobiose. *Proc. Natl. Acad. Sci. U.S.A.* **1998**, *95*, 5462−5467.
(55) Mallikaratchy, P.; Stahelin, R. V.; Cao, Z. H.; Cho, W.; Tan, W. H. Selection of DNA Ligands for Protein Kinase C-*δ*. *Chem. Commun.* **2006**, *30*, 3229−3231.
(56) Jellinek, D.; Green, L. S.; Bell, C.; Janjic, N. Inhibition of Receptor Binding by High-Affinity RNA Ligands to Vascular Endothelial Growth Factor. *Biochemistry* **1994**, *33*, 10450−10456.
(57) Tok, J. B. H.; Fischer, N. O. Single Microbead SELEX for Efficient ssDNA Aptamer Generation Against Botulinum Neurotoxin. *Chem. Commun.* **2008**, *28*, 1883−1885.
(58) Tang, Z. W.; Parekh, P.; Turner, P.; Moyer, R. W.; Tan, W. H. Generating Aptamers for Recognition of Virus-Infected Cells. *Clin. Chem.* **2009**, *55*, 813−822.
(59) Dwivedi, H. P.; Smiley, R. D.; Jaykus, L. A. Selection and Characterization of DNA Aptamers with Binding Selectivity to *Campylobacter Jejuni* Using Whole-Cell SELEX. *Appl. Microbiol. Biotechnol.* **2010**, *87*, 2323−2334.
(60) Park, S. Y.; Kim, S.; Yoon, H.; Kim, K.-B.; Kalme, S. S.; Oh, S.; Song, C. S.; Kim, D. E. Selection of an Antiviral RNA Aptamer Against Hemagglutinin of the Subtype H5 Avian Influenza Virus. *Nucleic Acid Ther.* **2011**, *21*, 395−402.
(61) Lee, Y. J.; Han, S. R.; Kim, N. Y.; Lee, S. H.; Lee, S. W. An RNA Aptamer that Binds Carcinoembryonic Antigen Inhibits Hepatic Metastasis of Colon Cancer Cells in Mice. *Gastroenterology* **2012**, *143*, 155−165.
(62) Wang, R. H.; Zhao, J. J.; Jiang, T. S.; Kwon, Y. M.; Lu, H. G.; Jiao, P. R.; Liao, M.; Li, Y. B. Selection and Characterization of DNA Aptamers for Use in Detection of Avian Influenza Virus H5N1. *J. Virol. Methods* **2013**, *189*, 362−369.


DOI: 10.1021/acsami.5b01180
*ACS Appl. Mater. Interfaces* 2015, 7, 11215−11223